HHS Public Access

Author manuscript

Exp Dermatol. Author manuscript; available in PMC 2020 April 01.

Published in final edited form as:

Exp Dermatol. 2019 April ; 28(4): 442–449. doi:10.1111/exd.13899.

Comparative regenerative biology of spiny (*Acomys cahirinus*) and laboratory (*Mus musculus*) mouse skin

Ting-Xin Jiang[1], **Hans I-Chen Harn**[1,2], **Kuang-Ling Ou**[1,3,4], **Mingxing Lei**[5,6], and **Cheng-Ming Chuong**[1,2,5]

[1]Department of Pathology, School of Medicine, University of Southern California, Los Angles, California, USA

[2]International Research Center of Wound Repair and Regeneration (iWRR), National Cheng Kung University, Tainan, Taiwan

[3]Ostrow School of Dentistry, University of Southern California, Los Angles, California, USA

[4]Divison of Plastic and Reconstructive Surgery, Department of Surgery, Tri-Service General Hospital, National Defense Medical Center, Taipei, Taiwan

[5]Integrative Stem Cell Center, China Medical University Hospital, China Medical University, Taichung, Taiwan

[6]Institute of New Drug Development, College of Pharmaceutical and Food Sciences, China Medical University, Taichung, Taiwan

Abstract

Wound-induced hair follicle neogenesis (WIHN) has been demonstrated in laboratory mice (*Mus musculus*) after large (>1.5 × 1.5 cm^2) full-thickness wounds. WIHN occurs more robustly in African Spiny mice (*Acomys cahirinus*), which undergo autotomy to escape predation. Yet, the non-WIHN regenerative ability of the spiny mouse skin has not been explored. To understand the regenerative ability of the spiny mouse, we characterized skin features such as hair types, hair cycling, and the response to small and large wounds. We found that spiny mouse skin contains a large portion of adipose tissue. The spiny mouse hair bulge is larger and shows high expression of stem cell markers, K15 and CD34. All hair types cycle synchronously. To our surprise, the hair cycle is longer and less frequent than in laboratory mice. Newborn hair follicles in anagen, are more mature than C57Bl/6 and demonstrate molecular features similar to C57Bl/6 adult hairs. The second hair cycling wave begins at week 4 and lasts for 5 weeks, then telogen lasts for 30 weeks. The third wave has a 6-week anagen, and even longer telogen. After plucking, spiny mouse hairs regenerate in about 5 days, similar to that of C57Bl/6. After large full-thickness excisional wounding, there is more de novo hair formation than C57Bl/6. Also, all hair types are present and

*Corresponding author: Cheng-Ming Chuong, M.D., Ph.D., Keck School of Medicine, University of Southern California, 2011 Zonal Ave, HMR 313B, Los Angeles, CA 90089, cmchuong@usc.edu.

Author Contributions

T.X.J. and C.M.C. conceived the idea and experimental design. T.X.J., H.I.H. and M.L. conducted the experiments. T.X.J., H.I.H., K.L.O. and C.M.C. prepared the manuscript.

Conflict of Interest

The authors declare that there are no conflicts of interest.

pigmented, in contrast to the unpigmented zigzag hairs in C57Bl/6 WIHN. These findings shed new light on the regenerative biology of WIHN and may help us understand the control of skin repair versus regeneration.

Keywords

spiny mouse; hair cycle; regeneration; wound healing; scar

Introduction

Successful wound repair usually ends with a scar that restores the continuity of injured tissue but which does not function like the original, uninjured tissue. Human adults are unique in our ability to "overheal" ourselves with hypertrophic or pathological scars.[1] Patients who underwent surgical procedures or had major trauma, especially burn injuries, suffered from disfiguring, sometimes painful, scarring which leads to permanent functional loss.[2] In contrast, regeneration, which means nearly total recapitulation of the original tissue architecture after injury, occurs in the African spiny mouse (*Acomys cahirinus*)[3] and is the ultimate goal of the clinical treatment of wounds. The repair of most injuries in human adults results in a patch of fibroblasts and disorganized extracellular matrix. *Acomys* can heal full-thickness skin wounds in a scar-free manner with the complete regeneration of hair follicles, sebaceous glands and dermis after skin autotomy induced by self-defense to escape predation.[3] Thus, *Acomys* provides a versatile model to study regeneration of mini-organs in skin. We can learn more about regeneration versus repair by comparing wound healing in *Acomys* with *Mus*.

As a mini-organ in skin, the hair follicle is composed of different layers and each of them encompasses numerous cell types characterized by specific programs of differentiation.[4] In addition to the delicate and complex structure, hair follicles also provide a unique stem cell niche so that they undergo regeneration and involution cycles.[5] There are four major stages of each hair cycle: anagen (growth), catagen (degeneration), telogen (rest) and exogen (shedding). The quiescence and activation of hair follicle stem cells drive the hair cycles.[6] In full-thickness skin wounds, stem cells also play an important role in restoration and repair of lost tissue. Moreover, while de novo hair follicle generation has never been observed in humans after injuries, wound-induced hair neogenesis (WIHN)[7] was found in the central area of the healing skin of adult mice (*Mus*). In the WIHN model, endogenous reprogramming occurs to generate not only new hair follicles but also sebaceous glands and dermal adipose tissue. Additionally, Plikus *et al.* showed the ability of wound myofibroblasts to convert to fat cells indicating the opportunity to influence regeneration over scarring after wounding.[8] Therefore, we also want to compare the WHIN model between *Acomys* and *Mus*.

To examine the similarities and differences in the morphology of *Acomys* and *Mus*, we compared their gross view, skin sections and hair types first.[9] Like *Mus*, *Acomys* has zigzag, awl and guard spiny hair. Second, we studied the hair cycle, regeneration cycle after shaving and plucking and skin section staining with epithelial and dermal stem cell markers (K15,

CD34 and Sox2). Unlike *Mus*, the hair cycle of *Acomys* begins before birth and is as long as 7–8 months after shaving. We observed that *Acomys* already has a fur coat and the hair follicles are in anagen status at birth. After hair plucking, *Acomys* regains hair follicles with full recovery in 20 days. Compared to *Mus*, *Acomys* has more K15, CD34 and Sox2 expressing cells in the hair follicle. Full-thickness skin excisional wounds ($1.5\times1.5cm^2$) in *Acomys* heal quickly (20 days for full closure) with all three types of *de novo* hair regeneration (occurring at 30 days in the periphery; 40 days in the wound center) and pigmentation. By comparing the response of *Acomys* and *Mus* to the WIHN model, we set to decipher how regeneration versus repair can be achieved. These data serves as the first step to study further fundamental principles to regeneration in and beyond the skin system.

Material and methods

Spiny mouse

African spiny mice, *Acomys cahirinus*, are from Dr. Malcolm Maden at the University of Florida and Dr. Ashley W Seifert of University of Kentucky. The mice are transferred to our facility through a MTA. A colony of captive-bred *Acomys cahirinus* was established at the University of Southern California (USC) and all experiments were performed with protocols approved by the USC IACUC. The spiny mice are fed on a mixed diet containing rabbit diet, sunflower seed and wild bird seed mix. C57Bl/6 mice are from the Jackson laboratory and fed a regular rodent diet. We use 3 to 6 month old adult female spiny mice for wound experiments unless otherwise specified. All mice used in this project were determined to be healthy by a USC veterinarian.

Histology and immunostaining

Mouse dorsal skin samples were dissected from different ages and fixed with 4% paraformaldehyde in PBS at 4°C for overnight followed by procedures described by Jiang and Chuong[10] for histology and immunohistochemistry. Paraffin section immunostainings were performed using following primary antibodies: Mouse anti-K14 (1:200, Thermo Fisher, Cat# MA1–34677, RRID:AB_2134821), mouse anti-K10 (1:200, Thermo Fisher, Cat# 39–5300, RRID:AB_2533418), mouse anti-AE13 (1:200, Abcam, Cat# ab16113, RRID:AB_302268), mouse anti-AE15 (1:200, Santa Cruz, Cat# sc-80607, RRID:AB_2303435), rabbit anti-TRP63 (p63, 1:200, Santa Cruz, Cat# sc-8343, RRID:AB_653763), goat anti-K15 (1:500, Thermo Fisher, Cat# MA1–90929, RRID:AB_2132754), goat anti-CD200 (1:200, R&D systems, Cat# AF3355, RRID:AB_2073945), goat anti-Sox 2 (1:200, R&D systems, Cat# AF2018, RRID:AB_355110), rat anti-CD34(1:200, eBioscience, Cat# 14-0341-85, RRID:AB_467211), PCNA (1:200, Millipore Cat# CBL407, RRID:AB_93501), and mouse anti-MitfD5 (1:200, Abcam, Cat# ab3201, RRID:AB_303601). Whole mount immunostaining of mouse epidermis was performed with rabbit anti-K17 (1:200, Cell signaling technology, Cat# D32D9, RRID:AB_10830066). Color was developed with the peroxidase substrate AEC kit (Vector Labs, Burlingame CA) or visualized with fluorescent secondary antibodies.

Spiny mouse hair plucking

Spiny mouse hairs were plucked with wax stripping or forceps on anaesthetized animals. The proportion of hair types was evaluated by counting the total numbers of all de novo hairs in the wound, and comparing them to the hairs in a 1×1 cm2 square area of normal skin. The percentage is calculated based on the sum of all hair types in either the wound or the skin. Percentages of different hair types were collected from 3 different mouse wounds and normal dorsal skins. SD was calculated from 3 independent biological samples (N=3). More than 400 hairs were calculated in each sample.

Spiny mouse wounding

Mice were anesthetized and a 1.5×1.5 cm^2 section of dorsal skin was excised. Ito et al[7] used a 1X1 cm^2 area as large wound model. Here, we optimized it from 1X1 cm^2 to 1.5×1.5 cm^2 because of the size of *Acomys* is larger than *Mus*.

Whole mount staining of spiny mouse wound epidermis and dermis

Wound epidermis was separated from dermis as reported by Ito et al[7]. Briefly, the specimens of full-thickness wounds were incubated in 20 mM EDTA in PBS at 37°C overnight. Epidermis was gently peeled off from dermis with fine watchmaker's forceps and fixed in 1:4 DMSO/methanol for one hour and incubated with 3% H_2O_2 for 20 min. The specimen was washed with PBS, blocked with FBS for one hour and then incubated with rabbit anti-K17 antibody at 4°C overnight. After washing with PBS, the secondary antibody was added and incubated for another one hour at room temperature. The specimen then was washed with PBS again and color developed using AEC kit (Vector Labs, Burlingame CA). The dermis was fixed in acetone at 4°C for overnight, rinsed with PBS and then incubated in NBT/BCIP to develop color.

Results

Spiny mice show distinct hair types, with different ratios in different body regions.

The adult spiny mouse shows different hair types and color on its dorsal (Fig. 1A1), lateral (Fig. 1A2) and ventral (Fig. 1A3) skin. The dorsal hairs are brown, the lateral hairs are lighter and more yellowish than those in the dorsum, and the ventral hairs are white. H&E sections show that spiny mouse skin contains a very high proportion of adipose tissue (~85% of full thickness) regardless of its location on the body (Fig. 1B1–B3). The spiny hairs (awl hairs) are thick and have a large hair bulge (Fig. 1B1'–B3'). Dimension wise, dorsal hairs are the longest and thickest, followed by lateral and lastly ventral. All hair types can be found in dorsal, lateral and ventral parts of the spiny mouse skin (Fig. 1C1–C3); however, they differ in percentage. The hair type percentages in the order of guard, awl and zigzag hairs are 18%, 33%, and 49% (total hair = 473 hairs/cm^2) in the dorsum, 6%, 41%, and 53% (total hair = 854 hairs/cm^2) in the flank, and 2%, 43%, and 55% in the ventral skin (total hair = 1060 hairs/cm^2), respectively (Fig. 1D). Using Student's t-test, we found it significantly different ($P<0.01$) for each hair type between each sample (N=3) in the dorsal, flank and ventral regions.

Hair follicle stem cell markers CD34 and K15 are highly expressed in the bulge region of adult spiny mouse hairs.

We perform immunohistochemistry to characterize the expression pattern of skin and stem cell markers in adult spiny mouse skins. K10, a marker for differentiated keratinocytes, is only expressed in the suprabasal layer of spiny mouse skin. AE15, a marker for inner root sheath cells, and AE13, a marker for upper hair cuticle cells, are not expressed in spiny mouse telogen hair follicles. CD200, a hair germ marker, is expressed in the hair follicle upper bulge. The basal layers of skin and hair follicles stain positively for K14 and p63. Furthermore, hair stem cell markers CD34, K15 and Sox2 are highly expressed in the bulge of all 3 hair types. Sox2, in particular, is indeed expressed in the bulge region (red arrow) and dermal papillae (red arrow head) of telogen hairs, but in anagen phase is only expressed in the dermal papillae (Fig. 1F, F').

The spiny mouse shows slower hair cycling, and all hair types cycle synchronously.

The spiny mouse pup is born with a fur coat that exhibits all 3 hair types in anagen (Fig. 2A, A', A"), indicating the spiny mouse hairs start to grow in the embryo. We shaved the dorsal hair of the 2-week-old mouse to observe hair growth, and found the first hair wave persists past week 2 as it enters early catagen (Fig. 2B, B', B"), but the posterior part of the skin is still visibly darker than the anterior side (Fig 2B, blue bar). This initial hair wave ceases 3 weeks after birth (Fig. 2C, C', C"). All hair types, guard, awl and zigzag, cycle synchronously. The second hair cycle wave begins on week 4, starting from the dorsal mid-body region (Fig. 2D). While most of the dorsal skin is still in early anagen, the anterior part of the skin (Fig. 2D arrowhead, 2D') is at an earlier hair cycle stage than the posterior side (Fig. 2D double arrowhead, 2D"). On week 6, the hair fibers are visibly thicker, and the skin also contains a thick adipose layer (Fig. 2E, E', E"). On week 8, most of the dorsal skin of the mouse is in anagen except for the neck region (Fig. 2F. orange bar). Zigzag (Fig. 2F' arrowhead), guard (Fig. 2F" arrow) and awl (Fig. 2F" asterisk) hairs from the mid-body region are all found in anagen. By week 10, most of the hairs have entered telogen (Fig. 2G), only the anterior dorsal skin near the neck is in catagen (Fig. 2G arrowhead, Fig. 2G'). The adipose tissue occupies the majority of the thickness during telogen (Fig. 2G"). In addition, this second hair wave coincides with the change in hair color, as the appearance of the newly grown hairs is brown (Fig. 2H). However, after shaving and revealing the hair close to the skin, the proximal end of the hairs appears to be gray (Fig. 2I, 9–13 wk), reflecting the differential pigmentation of the hair fiber in different body regions and locations along the hair fiber. These differences give rise to distinct color patterns on the dorsal, lateral and ventral sides. The third hair wave begins much later on week 42 through week 47 and telogen is even longer. This is evident from new hair growth on a shaved 3-month-old mouse (Fig. 2J, 40–45 wk, green bar). Generally speaking, the spiny mouse hair wave lasts around 6 weeks, with a long ~27-week gap between the second and third wave. The timeline of the spiny hair cycle is illustrated in Fig. 2K. While in C57Bl/6 mice, anagen occurs in complex domain patterns throughout different parts of the body after the first two synchronous cycles, in spiny mice, each hair wave does not fragment into domains but appears to be a coordinated, slow cycling wave, with a longer anagen, and a very long telogen phase.

Hair plucking initiates hair regeneration in spiny mice.

Here we plucked all the hairs within a 2 × 4 cm^2 area on the dorsal skin, and hence created micro-injuries to track hair regeneration after plucking (Fig. 3A). Gross-observation shows that mature hairs are visible 14 days after plucking (Fig. 3A, D14), and new hairs repopulated the plucked area after 20 days (Fig. 3A, D20). H&E sectioning of the skin shows new hair follicles began to regenerate as early as 5 days after hair plucking (Fig. 3B, D5), and these hairs mature to full size after 12 days (Fig. 3B, D12). Moreover, all hair types regenerated in sync and were observed on days 5, 7, and 12 after plucking. PCNA staining, a marker for cell proliferation, shows that cells were positive, though sparingly on day 5 after plucking. On days 7 and 12, most of the hair cells, including those in the infundibulum and the bulge region, were positive for PCNA (Fig. 3B. arrow: guard; arrowhead: zigzag; asterisk: awl.)

All hair types regenerate while awl and guard hairs are pigmented in WIHN of spiny mice.

Ito et al. demonstrated that C57Bl/6 mice have the ability to regenerate hairs in a large full-thickness wound, yet only zigzag hairs were observed.[7] Seifert et al. have shown spiny mice shed and regenerate their skin after wounding. To characterize the regenerative responses of the spiny mouse to a large wound, we created a 1.5 × 1.5 cm^2 wound on the dorsal skin of the spiny mouse and allowed it to heal by secondary intention. After approximately 35 days, we found that all 3 hair types were regenerated (Fig. 4A1–3). Comparatively, the original hair fibers (Fig. 4B, mid-upper panel) are still thicker than newly regenerated ones (Fig. 4B, mid-lower panel). Furthermore, the respective percentage of hair types (guard, awl, zigzag) remained very similar to unwounded skin (22%, 27%, 51% in regenerated hair vs. 20%, 35%, 45% in normal skin, Fig. 4B graph).

In response to wounding, the regenerated awl and guard hairs can be pigmented (Fig. 4C), while the zigzag hairs remain unpigmented. The hair placodes are positive for MitfD5, a marker for melanocytes, as early as 15 days after wounding (Fig. 4C1). MitfD5 localizes to the hair follicles 30 days after wounding, reflecting the role of melanocytes in regenerating pigmented hair fibers (Fig. 4C2). All three types of hairs are completely repopulated throughout the whole wound (Fig 4D, 4D1and 4D2). Six months after wounding, we plucked the regenerated new hairs. All three types of hairs grow back (Fig. 4E), which means de novo hair can recycle after being plucked.

Discussion

In this study, we characterized the spiny mice's skin tissue, hair fiber types, molecular expression, hair cycle pattern, and its response after hair plucking or wounding. Compared to laboratory mice (*Mus*), the spiny mouse skin contains a very large portion of adipose tissue in the hypodermis (Fig. 2). The spiny hair fibers are thicker and longer, and the percentage of hair type is different from *Mus* (18% guard, 33% awl, 49% zigzag in *Acomys*, vs 2% guard, 6% auchene, 7% awl and 85% zigzag in *Mus*) (Fig.1).[11] The hair bulges are larger and show high expression of stem cell markers K15, CD34 and Sox2 (Fig. 1). The *Acomys* skin undergoes 2 rounds of rapid hair cycles starting from embryonic day 24,[12] in contrast to post-natal day 3 in *Mus*. This can be attributed to the precocial nature of spiny

mice; though the time points seem different (hair grows in *Acomys* before birth and in *Mus* after birth), they are actually in the same hair cycle. The hair cycle period is longer in *Acomys* than *Mus*. The anagen in *Acomys* each lasts around 5–6 weeks, and telogen of the first three hair cycles is 2 weeks, 30 weeks and even longer, respectively (Fig. 2). Interestingly, when observing the spatiotemporal pattern of hair cycling in the spiny mice, we noted that there were no complex hair cycle domain patterns as previously observed in C57Bl/6 mice,[13, 14] which suggests a higher threshold to activate telogen to anagen transition for spiny mouse hairs. We have learned that this domain pattern is regulated by BMP4 from intradermal adipose tissue that inhibits Wnt/β-catenin signaling in the skin. We speculate that this "less restricted" hair wave observed in the spiny mice may imply less local dermal control and allows a more robust response to occur across the skin during homeostasis and regenerative wound healing. We will need to characterize intradermal adipose tissue in the spiny mouse to see if they also express cyclic BMP4 expression.[12]

It is intriguing that, compared to *Mus* dermal white adipose tissue (dWAT) in telogen, which reduces in size by ~50%,[15] there is no obvious thinning of the thick adipose layer in *Acomys* skin. In this review article, Guerrero-Juarez and Plikus[15] report evidence that dermal adipocytes are heterogenous in development, in sensitivity to catagen and spatial arrangement. We speculate that: 1) only a relatively small portion of the hypodermis adipose tissue responds to HF cycling in Acomys, and 2) the adipose layer maintains its thickness at all times which may aid in wound healing. Due to the fragile nature of the Acomys skin, it becomes imperative for the skin to maintain its niche for fast regeneration, and hence this adipose tissue layer is uncoupled with HF cycling. These interesting possibilities will require further investigation. Furthermore, a better microenvironment provided by the thickened adipose tissue may be an important reason underlying spiny mouse's regenerative ability. Previous studies have identified reciprocal signaling that takes place between dWAT and hair follicles to regulate their progression through cycle stages. Anagen hair follicles secrete multiple BMP ligands and activate transcription regulator Zfp423, which is necessary for adipogenesis in skin. In telogen, dWAT expresses BMP2, which maintains hair follicle stem cells in a quiescent state, to prevent hair over production on the skin. Considering the long telogen in *Acomys*, it is plausible that BMP2 may play a role and further characterization is required in future study.

Several previous reports have tried to unravel the mechanism behind the spiny mice's superior ability to regenerate after wounding.[3, 12, 16–18] Brant *et al.* have analyzed and compared the gene expression profiles during skin regeneration in *Mus* and *Acomys*, and identified the differences in the extracellular matrix profiles. *Mus* wounds express high levels of TIMP1 and low levels of Fn1, MMP9, and MMP13 and a high collagen I to III ratio. In contrast, *Acomys* wounds express high Fn1, MMP9 and MMP13 and a high collagen III to I ratio.[3, 19,20] On a side note, these results are based on gene expression data generated from microarrays and RT-PCR data, and from cytokine arrays all designed for mouse. However, Simkin et al., pointed out the shortcomings of comparing across species by microarray data analysis. To further explore the differences in molecular expression between *Mus* and *Acomys*, Gawriluk et al. acquired RNA-seq data.[21] Many of the findings of Brant *et al.* were also observed in the transcriptome analysis with the exceptions of Fn1 which was

high in *Mus* and low in *Acomys* and collagen III which is expressed to higher levels in *Mus* than in *Acomys*. The spiny mouse genome should be publicly available in early 2019.

The spiny mouse wounds are described to have a profile more similar to fetal wounds.[17] The immune responses of the two species are also rather different. *Mus* expresses high interleukins (IL), CXCLs, MCPs and CSFs, while the cytokine responses in *Acomys* is generally low, IL-1 and MIP-1 being the only exception.[17, 19] Hair plucking in *Mus* also activates Ccl2, Cxcl2, and IL-1, and initiates hair wave and hair regeneration.[22] In *Acomys*, our study shows all 3 hair types begin to regenerate as early as 5 days after plucking (Fig. 3). Despite the seemingly similar ability to heal a small wound (<6 mm), Seifert *et al.* have shown that the spiny mice can close a 6 mm wound rapidly, and the wound bed is characterized by low expression of myofibroblasts, a stark contrast to the normal response of a *Mus*.[3] Lastly, although Ito *et al.* successfully demonstrated that *Mus* can regenerate hair by WIHN,[7] and other investigations identified additional regulatory factors,[8, 23, 24] WIHN in *Mus* has not yet shown: 1) regeneration of hair types other than zigzag, 2) pigmentation of regenerated hairs, and 3) *de novo* hair follicles that cover the entire wound bed, as observed in this study. The comparison is summarized in Table 1.

Why does the spiny mouse skin contain a thick layer of adipose tissue? Seifert *et al.* show that the spiny mouse skin is weak, very deformable and tears easily.[3] We postulate the high adipose content in skin partially contributes to this mechanical characteristic, as the ultimate tensile strength of obese mouse skin is much lower to that of lean mice (45.9 vs. 107 N/cm^2).[25] Although adipose tissue seems to constitute only a small portion of the regenerated wound (Fig. 4C), it has been identified as an important regulator of hair follicle growth.[26] Adiponectin-deficient mice showed severely delayed re-epithelialization, and cultured keratinocytes treated with adiponectin showed increased proliferation and migration,[27–29] suggesting adipokines are essential for normal wound healing. Moreover, regenerative healing has been shown to be heavily age-dependent,[30–32] and signals from the adipose tissue also modulate hair stem cell behavior and aging.[33]

Another remarkable observation is the regeneration of pigmented de novo hairs. In the standard Mus WIHN model, 3–4 week old mice were used, in which little to no regenerated hairs were pigmented as reported.[7, 23] However, Yuriguchi et al. used 5 week old mice and created wounds on the anagen skin and observed pigmented regenerated hairs. They attribute this pigmentation to the elevated level of Wnt7a in keratinocytes during anagen, which may direct melanocyte stem cells to produce pigmented hairs in the regenerated follicles. This notion was supported by the finding that Kitl (melanocyte stimulatory factor) expressing transgenic mice regenerated pigmented hairs regardless of age or hair cycle stage.[34] While we still do not have a clear mechanism, the high proportion of adipose tissue, enlarged bulge and high expression of hair stem cell markers CD34, K15 and Sox2 may provide important clues. The development of the thick and spiny awl hair in the spiny mouse is attributed to hair cells undergoing an additional step of proliferation and differentiation.[12] We postulate the presence of stem cell marker-positive cells around the hair bulge probably facilitated cell proliferation (via p63) and differentiation (via Sox2, CD34 and K15) to allow pigmented hairs of all types to regenerate, which include the essential interaction and activation of MitfD5 positive cells.

In summary, by characterizing the African spiny mouse, this study shows its unique skin composition, molecular expression, hair cycle, and response to wounding. Surprisingly, the normal hair cycle is not faster and more frequent; rather it is longer and slower. All three hair types cycle synchronously, suggest the cycling is under a local dermal control, not autonomously in each hair follicle or each type of hair follicle. The slow progression of simple waves, in contrast to the complex hair domains in C57Bl/6,[13] suggest a different local dermal control. The facts that all three hair types form and they are pigmented suggest there may be different molecular mechanisms, different paths for cells to achieve de novo hair formation. Though further studies focusing on the molecular and even mechanical signaling would be necessary to reveal its mechanism, this study provides fundamental characteristics and clues to understand how to elicit regenerative wound healing.

Acknowledgments

This project is supported by NIH grant NIH GM125322 and AR 060306, the International Center for Wound Repair and Regeneration at National Cheng Kung University from The Featured Areas Research Center Program within the framework of the Higher Education Sprout Project by the Ministry of Education (MOE) in Taiwan, and by the grant of the Ministry of Science and Technology (MOST 107–3017-F-006–002) in Taiwan. The authors would like to thank Dr. Seifert and Dr. Maden for providing the spiny mice. We thank Dr. R. B. Widelitz for editing the manuscript.

References

[1]. Longaker MT, Gurtner GC, Semin. Cell Dev. Biol 2012, 23, 945. [PubMed: 23059792]

[2]. Aarabi S, Longaker MT, Gurtner GC, PLoS Med. 2007, 4, e234. [PubMed: 17803351]

[3]. Seifert AW, Kiama SG, Seifert MG, Goheen JR, Palmer TM, Maden M, Nature 2012, 489, 561. [PubMed: 23018966]

[4]. Schneider MR, Schmidt-Ullrich R, Paus R, Curr. Biol 2009, 19, R132. [PubMed: 19211055]

[5]. Plikus MV, Widelitz RB, Maxson R, Chuong CM, Int. J. Dev. Biol 2009, 53, 857. [PubMed: 19378257]

[6]. Hsu YC, Li L, Fuchs E, Nat. Med 2014, 20, 847. [PubMed: 25100530]

[7]. Ito M, Yang Z, Andl T, Cui C, Kim N, Millar SE, Cotsarelis G, Nature 2007, 447, 316. [PubMed: 17507982]

[8]. Plikus MV, Guerrero-Juarez CF, Ito M, Li YR, Dedhia PH, Zheng Y, Shao M, Gay DL, Ramos R, Hsi TC, Oh JW, Wang X, Ramirez A, Konopelski SE, Elzein A, Wang A, Supapannachart RJ, Lee HL, Lim CH, Nace A, Guo A, Treffeisen E, Andl T, Ramirez RN, Murad R, Offermanns S, Metzger D, Chambon P, Widgerow AD, Tuan TL, Mortazavi A, Gupta RK, Hamilton BA, Millar SE, Seale P, Pear WS, Lazar MA, Cotsarelis G, Science 2017, 355, 748. [PubMed: 28059714]

[9]. Muller-Rover S, Handjiski B, van der Veen C, Eichmuller S, Foitzik K, McKay IA, Stenn KS, Paus R, J. Invest. Dermatol 2001, 117, 3. [PubMed: 11442744]

[10]. Jiang TX, Chuong CM, Dev. Biol 1992, 150, 82. [PubMed: 1371480]

[11]. Chi W, Wu E, Morgan BA, Development 2013, 140, 1676. [PubMed: 23487317]

[12]. Montandon SA, Tzika AC, Martins AF, Chopard B, Milinkovitch MC, Evodevo 2014, 5, 33. [PubMed: 25705371]

[13]. Plikus MV, Mayer JA, de la Cruz D, Baker RE, Maini PK, Maxson R, Chuong CM, Nature 2008, 451, 340. [PubMed: 18202659]

[14]. Plikus MV, Chuong CM, J. Invest. Dermatol 2008, 128, 1071. [PubMed: 18094733]

[15]. Guerrero-Juarez CF, Plikus MV, Nat. Rev. Endocrinol 2018, 14, 163. [PubMed: 29327704]

[16]. Matias Santos D, Rita AM, Casanellas I, Brito Ova A, Araujo IM, Power D, Tiscornia G, Regeneration (Oxf) 2016, 3, 52. [PubMed: 27499879]

[17]. Brant JO, Lopez MC, Baker HV, Barbazuk WB, Maden M, PLoS ONE 2015, 10, e0142931. [PubMed: 26606282]

[18]. Harn HI, Ogawa R, Hsu CK, Hughes MW, Tang MJ, Chuong CM, Exp. Dermatol 2017, DOI: 10.1111/exd.13460.

[19]. Brant JO, Yoon JH, Polvadore T, Barbazuk WB, Maden M, Wound Repair Regen. 2016, 24, 75. [PubMed: 26606280]

[20]. Gawriluk TR, Simkin J, Thompson KL, Biswas SK, Clare-Salzler Z, Kimani JM, Kiama SG, Smith JJ, Ezenwa VO, Seifert AW, Nat. Commun 2016, 7, 11164. [PubMed: 27109826]

[21]. Simkin J, Seifert AW, Stem Cells Transl. Med 2018, 7, 220. [PubMed: 29271610]

[22]. Chen CC, Wang L, Plikus MV, Jiang TX, Murray PJ, Ramos R, Guerrero-Juarez CF, Hughes MW, Lee OK, Shi S, Widelitz RB, Lander AD, Chuong CM, Cell 2015, 161, 277. [PubMed: 25860610]

[23]. Nelson AM, Reddy SK, Ratliff TS, Hossain MZ, Katseff AS, Zhu AS, Chang E, Resnik SR, Page C, Kim D, Whittam AJ, Miller LS, Garza LA, Cell Stem Cell 2015, 17, 139. [PubMed: 26253200]

[24]. Gay D, Kwon O, Zhang Z, Spata M, Plikus MV, Holler PD, Ito M, Yang Z, Treffeisen E, Kim CD, Nace A, Zhang X, Baratono S, Wang F, Ornitz DM, Millar SE, Cotsarelis G, Nat. Med 2013, 19, 916. [PubMed: 23727932]

[25]. Enser M, Avery NC, Diabetologia 1984, 27, 44. [PubMed: 6468798]

[26]. Shook B, Rivera Gonzalez G, Ebmeier S, Grisotti G, Zwick R, Horsley V, Annu. Rev. Cell. Dev. Biol 2016, 32, 609. [PubMed: 27146311]

[27]. Jin CE, Xiao L, Ge ZH, Zhan XB, Zhou HX, Genet. Mol. Res 2015, 14, 8883. [PubMed: 26345819]

[28]. Salathia NS, Shi J, Zhang J, Glynne RJ, J. Invest. Dermatol 2013, 133, 812. [PubMed: 23096717]

[29]. Shibata S, Tada Y, Asano Y, Hau CS, Kato T, Saeki H, Yamauchi T, Kubota N, Kadowaki T, Sato S, J. Immunol 2012, 189, 3231. [PubMed: 22904306]

[30]. Chen CC, Murray PJ, Jiang TX, Plikus MV, Chang YT, Lee OK, Widelitz RB, Chuong CM, J. Invest. Dermatol 2014, 134, 2086. [PubMed: 24618599]

[31]. Kim DJ, Mustoe T, Clark RA, Wound Repair Regen. 2015, 23, 318. [PubMed: 25817246]

[32]. Nishiguchi MA, Spencer CA, Leung DH, Leung TH, Cell Rep. 2018, 24, 3383. [PubMed: 30257200]

[33]. Chen CC, Plikus MV, Tang PC, Widelitz RB, Chuong CM, J. Mol. Biol 2016, 428, 1423. [PubMed: 26196442]

[34]. Yuriguchi M, Aoki H, Taguchi N, Kunisada T, J. Dermatol. Sci 2016, 84, 80. [PubMed: 27435302]

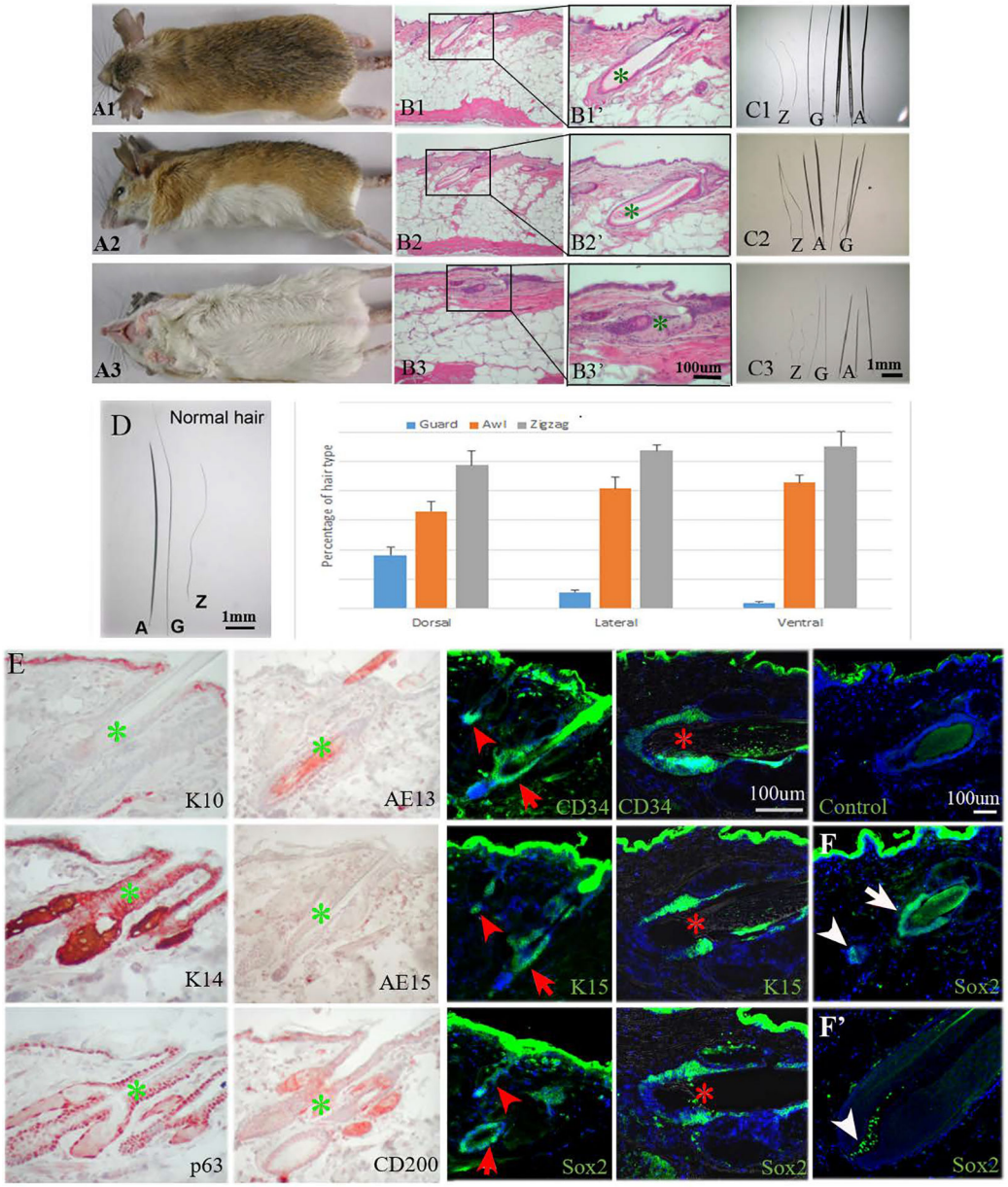

Fig. 1.

Spiny mouse hair types. A1. Dorsal view of adult spiny mouse with dark brown spiny hairs. A2. Lateral view of adult spiny mouse with yellow spiny coat. A3. Ventral view of adult spiny mouse with white spiny coat. B1, 2, and 3. H&E staining of dorsal, lateral, ventral spiny mouse skin. B1', B2', B3', the magnified view of B1, B2, and B3, respectively. C1, C2, and C3, all hair types (Z: zigzag hair; G: guard hair; A: awl hair) from dorsal, lateral and ventral side of the skin, respectively. D. The percentage of hair types from 1 cm^2 area of each respective body part. SD is calculated from 3 independent samples (N=3); more than 400 hairs are calculated in each sample. E. Immunostaining of K10, K14, p63, AE13, AE15, CD200, CD34, K15, and Sox2. Control: secondary antibody negative control. Arrowhead: zigzag hair; arrow: guard hair; asterisk: awl hair. F. Sox2 immunostaining of telogen and

anagen hair follicles. White arrow: hair bulge, arrowhead: dermal papilla. All photographs are representative of the data acquired from all specimens.

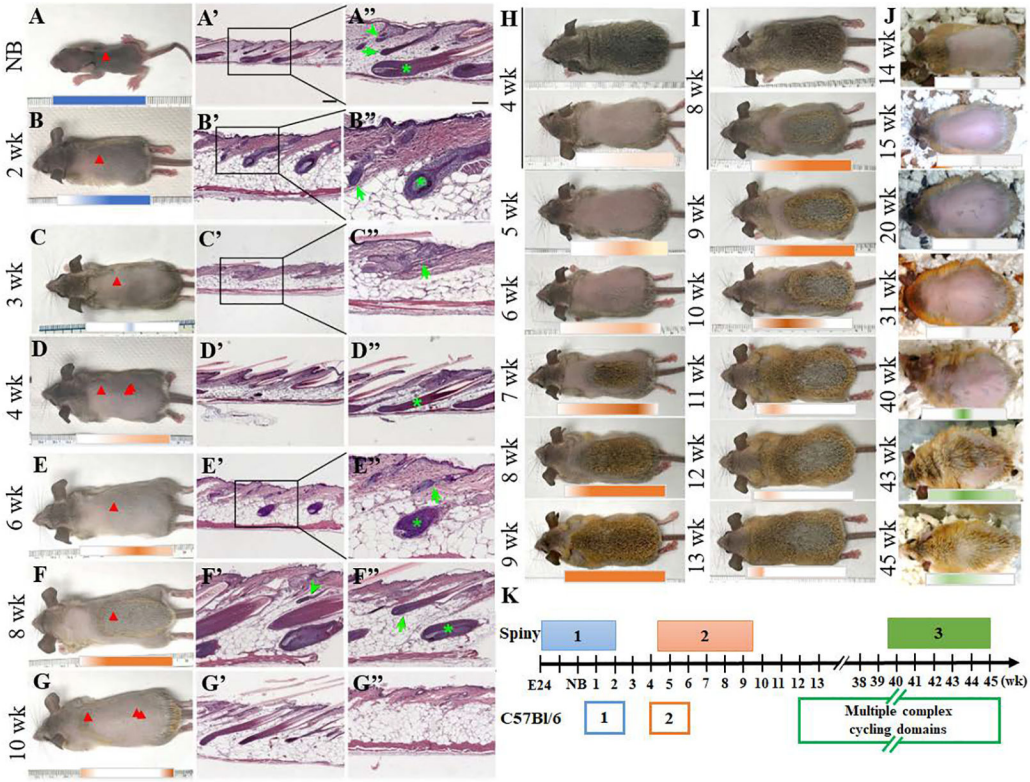

Fig. 2.

Spiny mouse hair cycle. A. The new born spiny mouse has a fur coat when it is born. (Red arrow indicates where the section was taken from. Arrowhead: zigzag hair; arrow: guard hair; asterisk: awl hair) A', A". H&E staining of skin section shows that all three hair types have developed in this stage. The hairs across the whole dorsal body are already in anagen at birth (red arrowhead, blue bar). B. This hair wave continues 2 weeks after birth (blue bar), but parts of the body (red arrowhead) begins to enter catagen (B', B"). C. Hairs were shaved at 3 weeks after birth. H&E staining showed that hairs have entered to telogen stage (arrowhead, C', C"). D. The spiny mouse hairs were shaved at 4 weeks after birth. D', H&E from red arrowhead, D", H&E from double red arrowhead, where the second hair waves start to regenerate, and hair stages are in exogen (D') and early anagen stages (D"). E, shaved 6-week-old mouse, in which hair waves begin to propagate from the mid-body region. E' and E", H&E from mid-body region (redarrowhead). F, shaved 8-week-old mouse. F' and F", the zigzag (green arrowhead), guard (green arrow) and awl (green asterisk) hairs are all in anagen stage. G, shaved 10-week-old mouse, end of hair wave. H&E section showing hairs in catagen (red arrowhead, G') and telogen (double red arrowhead, G"). Scale bar A', B', C', D', D", E', G', G", 200 um. A", B", C", E", F', F", 100 um. H. Hair wave propagation from 4 to 9 weeks. I. Hair wave sustaining from week 8 to week 13. J. The third wave did not start until 40 weeks after birth and lasted until 45th week (green bar). K. Comparison of hair cycle waves in spiny and C57Bl/6 mice. In C57Bl/6 mice, first two cycles are in general synchronous, and then they break into multiple complex cycling domains. In spiny mice, waves don't break into subdomains and the waves traverse the skin

more slowly, with longer anagen and very long telogen phases. All photographs are representative of the data acquired from all specimens.

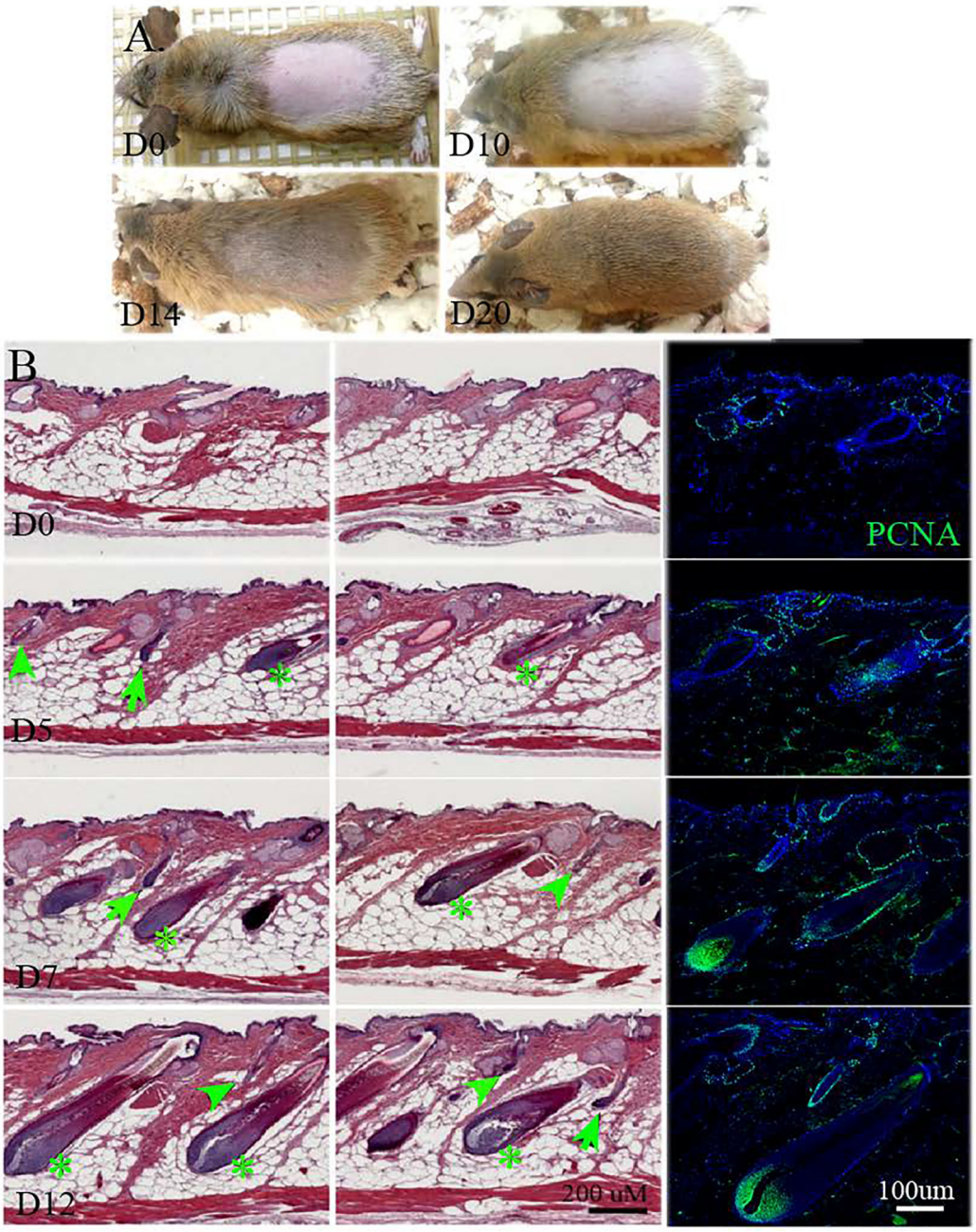

Fig. 3.

Spiny mouse hair regeneration after hair plucking. A. Spiny mouse hair was plucked and observed on day 0 (D0), day 10 (D10), day 14 (D14), and day 20 (D20). B. H&E staining of spiny mouse dorsal skin at 5, 7 and 12 days after hair plucking. Noted all hair types regenerated after plucking. Immunofluorescent PCNA staining shows proliferation during the hair cycle. Arrowhead: zigzag hair; arrow: guard hair; asterisk: awl hair. All photographs are representative of the data acquired from all specimens.

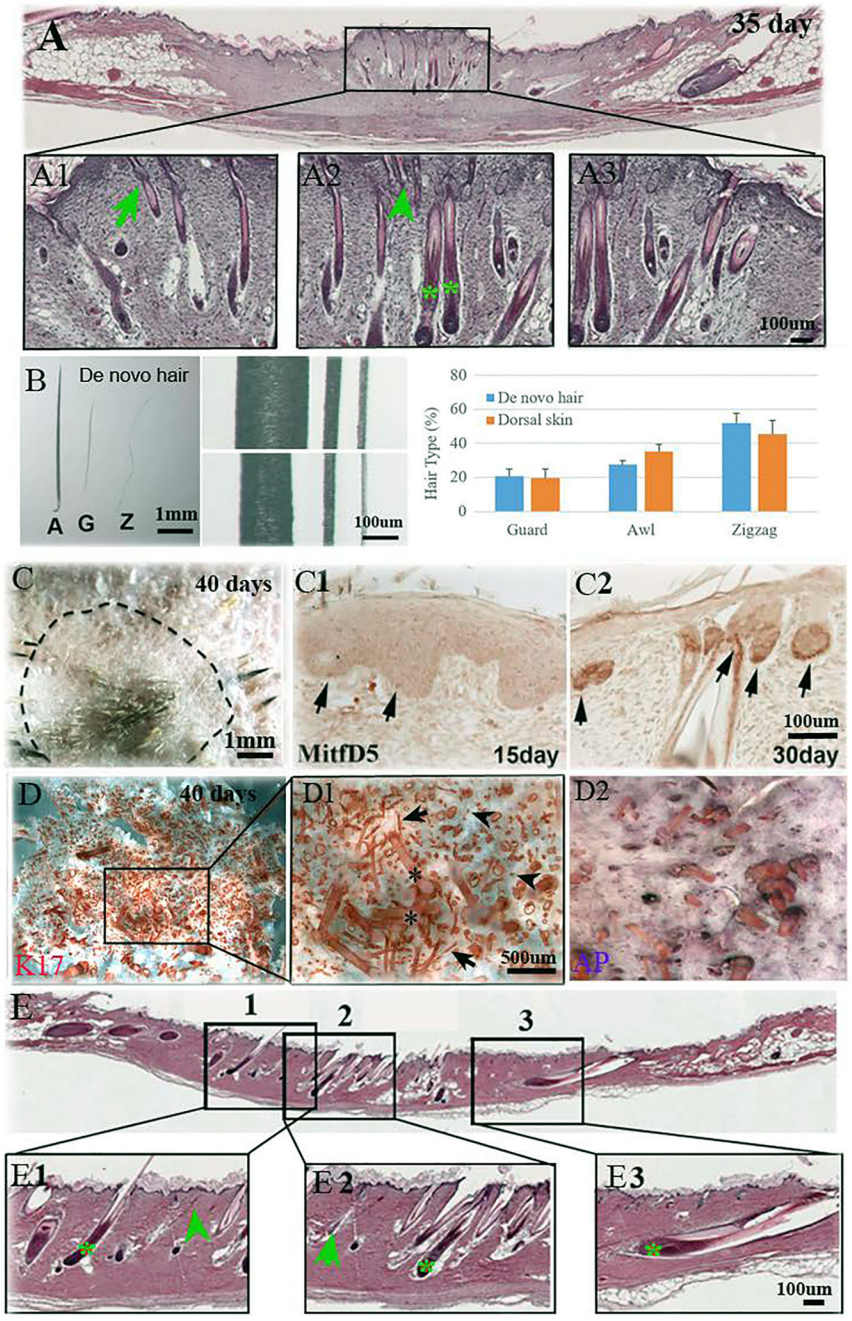

Fig. 4.

Regeneration of hair type, pigmentation and recycle. A. All three hair types, zigzag (A1, arrowhead), guard (A2, arrow), and awl (A3, asterisk) are regenerated 35 days after large 1.5×1.5 cm^2 wounding. B. The morphology of regenerated hairs. (A, awl; G, guard; Z, zigzag). The normal hairs (mid-upper panel) are thicker than regenerated hairs (mid-lower panel). The percentage of the *de novo* hair types is similar to the normal skin hair (B, graph). SD is calculated from 3 independent wounds and normal mouse dorsal skin samples (N=3). C. The pigmented hair shaft can be observed 40 days after wounding. Dotted line: original wound margin. C1. MitfD5 immuno-reactivity was expressed 15 days after wounding in hair

placodes (arrows). C2. MitfD5 immuno-reactivity was expressed in new hair follicles after 30 days (arrows). D. Wholemount staining of the wound epidermis and dermis (D, D1, D2) show regeneration of all hair types across the wound bed. Arrowhead: zigzag; arrow: guard; asterisk: awl. E. Six months after wounding, the regenerated hairs are plucked. All three hair types, zigzag (arrowhead), guard (arrow), and awl (asterisk) grow back.

Table 1.

Comparison of skin characterization and regenerative response to wounding in Mus and Acomys mice

	Mus	*Acomys*	References
Skin tissue	Epidermis, dermis, and hypodermis with a thin layer of adipose tissue.	Epidermis, dermis and a very thick portion of adipose layer in the hypodermis.	Fig. 1
Hair types	2% guard, 6% auchene, 7% awl, 85% zigzag.	18% guard, 33% awl, 49% zigzag in dorsum skin. All 3 hair types are thicker and longer. Awl hairs undergo a second round of anisotropic proliferation during growth.	[11, 12], Fig. 1
HFSC markers	Lower K15, CD34, Sox2 expression in adult hair follicles.	High expression of K15, CD34 and Sox2 in the large hair bulges.	Fig. 1
Hair cycle	1st hair cycle ends synchronously at about 3 weeks of age. 2nd hair cycle ends about 7 weeks of age. Complex hair cycle domains form after 2 months.	All hair types cycle synchronously. 1st hair cycle ends at about 3 weeks of age. Anagen of the 2nd hair cycle occurs between 4–9 weeks followed by a long telogen (until 38 weeks). Anagen of the 3rd hair lasts from 39–45 weeks followed by a very long telogen. No complex hair cycle domains are observed.	[5, 12], Fig. 2
In response to wounding			
ECM	High collagen I to collagen III ratio*, high TIMP1. Lower Fn1*, MMP9, MMP13. (*controversial)	High collagen III to collagen I ratio*, High Fn1*, MMP9, MMP13. (*controversial)	[3, 17, 20]
Immune	High ILs, CXCLs, MCPs, CSFs, etc.	Low cytokines, macrophages, high IL-1, high MIP-1. Lower CD86+.	[19, 20]
Hair plucking	Ccl2, Cxcl2, IL-1 activation, initiation of hair wave, and hair regeneration on day 5.	Regeneration of all 3 hair types beginning on day 5.	[22], Fig. 3
Small wound	More myofibroblasts, scarring. Direct contraction to close the wound.	Rapid wound closure, fewer myofibroblasts. Regeneration of all hair types.	[3]
Large full thickness wound (WIHN)	Regeneration of zigzag hair only. Incomplete coverage of wound bed. Pigmented regenerated hairs only from wounds created on 5 week old anagen skin regenerated hairs.	Faster regeneration of all 3 hair types and they can recycle after plucking. Complete repopulation of wound. Normal pigmentation in awl and guard regenerated hairs.	[7, 34], Fig. 4